Journal of Building Engineering 60 (2022) 105166

Contents lists available at ScienceDirect

Journal of Building Engineering

journal homepage: www.elsevier.com/locate/jobe

Detection of setting time during cement hydration using ground penetrating radar

Liyu Xie [a], Zihan Xia [a], Songtao Xue [a,b], Xiaoli Fu [c,*]

[a] Department of Disaster Mitigation for Structures, Tongji University, Shanghai, China
[b] Department of Architecture, Tohoku Institute of Technology, Sendai, Japan
[c] Department of Hydraulic Engineering, Tongji University, Shanghai, China

ARTICLE INFO

Keywords:
Setting time
Cement hydration
GPR
Non-contact monitoring
Passive wireless

ABSTRACT

The setting time of concrete needs to be detected to ensure the construction quality control. This research provides a new non-contact, nondestructive remote sensing detection method based on ground penetrating radar (GPR) for monitoring cement setting time. The moisture content of cement paste decreases during hydration, resulting in a change of its dielectric constant. Furthermore, dielectric permittivity affects the wave velocity and echo intensity of electromagnetic waves. Based on these characteristics, this paper utilizes GPR to measure the moisture content of cement paste in terms of changing dielectric permittivity, and then assess the setting time depending on the link between the moisture content and setting state of the cement paste. To detect an object smaller than one-wavelength, the full-waveform inversion is used to analyze the GPR echo data instead of the traditional velocity inversion measurement. The positive correlation between the reflection coefficient and dielectric constant is verified by both simulations and experiments. The experiment results accurately determine the initial and final setting time of cement paste, compared with the Vicat apparatus test. The method of GPR monitoring cement paste setting time based on full-waveform inversion theory can solve the quality control problems of concrete leveling automation and concrete layered construction automation.

1. Introduction

Concrete, defined as a mixture of a certain proportion of water, cement, sand and gravel conserved in a given environment, is a prevalent construction material in modern times [1]. Banfield [2]notes that despite concrete's broad range of applications and excellent performance, it is accompanied by various problems during actual construction, such as wall cracking, crusting, concrete bleeding, and abnormal concrete setting. He also states that abnormal setting will deteriorate the concrete strength, and this deterioration largely depends on the thoroughness of cement hydration in both ordinary concrete and high-strength concrete.

Slow setting, fast setting, and false setting are the three types of abnormal concrete settings. Concrete pouring difficulties will arise as a result of fast and false settings. A slow setting will lead to an insufficient early strength in concrete and a prolonged period of dismantling forms. The monitoring of setting state is of great significance in engineering [3]. During construction, the mass concrete leveling and compacting needs cement mortar to lose fluidity; that is, the fresh concrete after placing in the forms should reach the initial setting before the concrete surface is leveled and compacted. Conventionally, this process is done by workers with mechanical equipment, and the setting state is usually judged by the engineering instinct, which largely depends on the engineer's expertise.

* Corresponding author.
E-mail address: xlfu@tongji.edu.cn (X. Fu).

https://doi.org/10.1016/j.jobe.2022.105166
Received 11 May 2022; Received in revised form 21 July 2022; Accepted 19 August 2022
Available online 27 August 2022

Besides, construction personnel need to inspect the concrete regularly during the curing process to control concrete humidity and temperature, so that normal or accelerated hardening can occur as well as an increase in strength.

The curing of concrete is the process of cement hydration in a suitable environment. Hydration in concrete is mainly the reaction of clinker minerals in cement with water. The macroscopic phenomenon of hydration is a concrete setting, representing the transition process of new concrete from a liquid to solid phase. Conventionally, the hydration thoroughness can be judged by the concrete's setting time. With an accurate detection of setting time, construction engineers can schedule the transportation, placing, and curing appropriately, avoiding the generation of substandard concrete [4]. In laboratory experiments, scholars often use cement paste as an alternative sample to evaluate the process of hydration [5].

Usually, the setting state of concrete is manually tested by the manually operated standard Vicat apparatus for quality inspection due to its low cost [6,7]. This process often requires experienced workers to operate manually and takes a certain time for one measurement. To improve it, experts developed an automated version of Vicat apparatus for continuous inspection [8]. However, this does not change the disadvantages of the Vicat apparatus test. It can only measure a single sample at one time and need to flip the sample after initial setting manually. In addition, the price of automatic Vicat apparatus is more than 25 times that of conventional Vicat apparatus.

Aside from traditional detection methods, scholars began to study nondestructive testing methods for concrete setting state evaluations. Several measurement schemes were proposed based on different sensing mechanisms, electrical resistivity measurements, nuclear magnetic resonance (NMR), patch antenna sensors [9,10], and the ultrasonic wave transmission method [11]. Li et al. [12] used a non-contact resistivity meter based on the principle of transformer to establish a quantitative relationship between the concrete setting time and the critical point of resistivity. The resistivity curves obtained during the concrete setting revealed two critical locations of the initial and ultimate coagulation phases.

Toropovs et al. [13] employed neutron radiography to assess the humidity distribution in high-performance concrete. Different moisture content imitates radiant attenuation, which is eventually represented as humidity dispersion within concrete. She et al. [14] used nuclear magnetic resonance to monitor the hydration process and microstructure evolution of ordinary Portland cement (OPC) paste. The relaxation behavior of a large number of hydrogen nuclei (protons) in water was studied using NMR with a strong static magnetic field. NMR relaxation signals may offer information on the water molecule state and content, which can reveal the microstructure development of cement paste. Yi et al. [15] placed a patch antenna sensor in cement to determine the initial and final setting time during hydration. The moisture content variation can alter the dielectric constant of surrounding cement and eventually, the resonant frequencies of antennas. Trtnik et al. [16] investigated the link between initial setting time and ultrasonic propagation parameters of cement paste using ultrasonic wave transmission. The first setup time is based on the first inflection point on the ultrasonic pulse velocity curve.

For these aforementioned methods, concrete or cement paste needs to be in direct contacted with the sensing device for measurement. Repeated measurements require an electrical resistivity measurement probe, nuclear magnetic resonance sample collecting device, and ultrasonic measurement probe to adhere to the difficult-to-clean cement paste. The contamination on the probes will lower the measurement accuracy and influence future measurement results. On the other hand, the embedded patch antenna sensor must be connected with a Vector Network Analyzer (VNA) through a coaxial line to interrogate the resonance frequency to determine the concrete setting state.

Ground penetrating radar (GPR) is a prevalent nondestructive testing technique to detect the state of materials without embedded probes. GPR is widely used in civil engineering, usually for pavement assessment [17,18] and crack monitoring [19,20]. The utility of GPR in examining concrete has also been proven [21]. The electromagnetic wave created by GPR will be reflected when it encounters an interface with impedance discontinuity along the propagation route, which is the basis for GPR's exploration of underground targets. Scholars have proposed GPR imaging methods and survey evaluations based on wave velocity measurement, which take advantage of the fact that wave velocity propagation in the medium is regulated by the medium's permeability and dielectric constant. GPR uses electromagnetic (EM) waves to assess several conditions, including the concrete structures of internal cavities and water content. Kaplanvural et al. [22] performed time-delay GPR measurements on C-30 concrete blocks that used the center frequency of a 2 GHz shielded GPR antenna to determine the volumetric water content of the C-30 concrete block. Liu et al. [23] used ground-penetrating radar (GPR) to measure the thickness of thinner layers of ice and snow beneath the ground by measuring the velocity of electromagnetic waves in the medium using single shot and multiple receiver methods for a better accuracy of speed measurements.

However, due to technical limitations and noise jamming, the measuring of wave velocity can be challenging for targets of size less than one wavelength. Thus, researchers began to investigate the inversion of medium parameters utilizing other information carried by echoed waves, such as phase, amplitude, and intensity. Kaplanvural et al. [24] investigated the link between changes in electromagnetic wave attenuation and concrete moisture content, which are connected to the direct and reflected wave amplitudes generated by the sample's decrease in moisture content. AL-Qadi et al. [25] proposed a signal processing technology for a full-waveform inversion (using echo amplitude instead of wave speed) to calculate the dielectric constant of the pavement layered medium. Compared to the wave velocity measurement method, the full-waveform inversion method can obtain the electrical parameters of an object that is smaller than the minimum resolution of the wave velocity measurement, such as the dielectric constant and conductivity, resulting in an enhanced measurement resolution.

Higher precision monitoring can be achieved by using the full-waveform inversion approach with GPR in the field of civil engineering construction. GPR is the solution of construction in-site monitoring, which can meet the requirements of a nondestructive, noninvasive and high-efficiency test method that uses high frequency electromagnetic waves to detect the state of concrete to ensure the quality control of automatic construction process [26–28]. This paper uses GPR to conduct non-contact and nondestructive

monitoring of the cement paste setting state. The full-waveform inversion approach was used to determine the moisture content and setting time of cement paste with a thickness of less than one-wavelength. The setting state of cement paste is identified by the variation in moisture content, which is the free water that does not reacted with the cement. The amount of free water in cement can be used to determine the setting time of cement.

With the detection of cement paste setting time by GPR, it can be used to evaluate the setting state of fresh concrete in mass concrete leveling and compacting and realize automatic concrete screeding without human interference [29], which overcoming the limitations of conventional Vicat apparatus's time-consuming, human resource consuming and discontinuous monitoring. Besides, The high-efficiency, non-invasive GPR measurement method can be well combined with automatic construction, which is an ongoing advance for saving the workforce and improving productivity [30–34]. For example, the determination of the setting state of fresh concrete is crucial to the quality control of dam concrete construction. In a stratified dam casting process, it's essential to accomplish the upper layer paving and pouring before the lower layer's initial setting time [35]. It will improve the quality of the interlayer combination and ensure that the upper has good bonding between the concrete mixture and the lower performance [36]. Therefore, it is imperative to evaluate the setting state of the concrete in a remote and fast way, without any probe embedded in the concrete. The full-waveform inversion theory-based GPR monitoring setting time approach is an excellent option to fulfill this demand.

The structure of this paper is as follows, Section 2 introduces the hydration process of concrete. Section 3 describes the detection mechanism. Section 4 presents the numerical simulation in HFSS. Section 5 provides the experimental design and the analysis of the experimental results. Section 6 ends with a conclusion and the prospect of future research plans.

2. Hydration process of concrete

A lot of research has been done on the cement hydration mechanism over the last few decades [37–39]. As soon as water is added to the cement, part of the water will immediately combine with the cement to form a cement gel. This part of the water is called bound water, and the remaining part that is not participating in the chemical reaction is called free water. According to Taylor [40], we can divide the early cement hydration into four periods: 1) the initial hydrolysis period, 2) the induction period, 3) the acceleration period, and 4) the deceleration period. In the initial hydrolysis period, cement reacts immediately after mixing with water, and the free water decreases rapidly. After the initial hydrolysis period, hydration enters the induction period because the hydration forms tri-calcium silicate (C_3S) cement gel on the surface of cement particles, which hinders the hydration. The protective layer on the surface of cement particles is not stable and will gradually dissolve until the cement paste reaches the initial setting state. The hydration then enters the acceleration period, when the previously dissolved protective layer reacts to form a more stable hydration production, C–S–H cement gel. In this process, a large amount of C_3S is consumed. When the C–S–H cement gel production reaches a certain level, the concrete strength will be formed initially, and the hydration reaction rate decreases. Then concrete reaches the final setting state, and the hydration enters a deceleration period.

In Fig. 1, the most common Portland cement is taken as an example, which is divided into three stages according to the changing trend of concrete moisture content over time during the hydration process. Stage I includes an initial hydrolysis period and induction period. Stage II is the hydration acceleration period, and Stage III is the hydration deceleration period.

In early cement hydration, free water is stably consumed, resulting in cement paste's constantly changing moisture content. Then, it is plausible to estimate the state of cement paste by the changing acceleration of moisture content in the cement paste, which can be defined as a derivative of the moisture content curve. The change in moisture content is also related to water evaporation. According to Xu [42], the evaporation rate of free water almost remains unchanged, which means we can ignore the influence of free water on the acceleration rate of water content. In Yi's paper [15], a method for judging the setting time by the moisture content is proposed. The moisture content acceleration change represents the rate of hydration. When the change rate of moisture content reaches a extreme

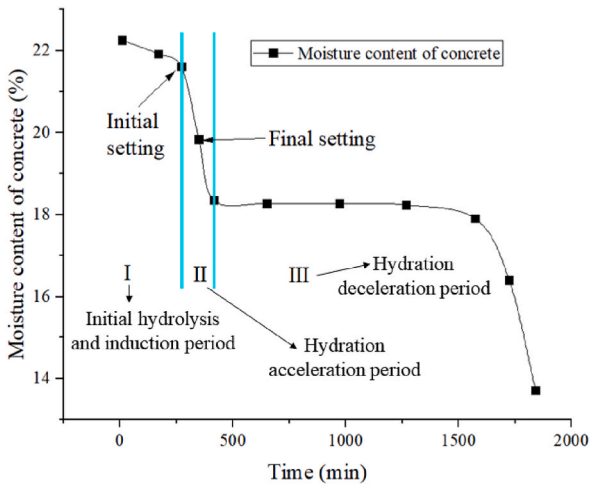

Fig. 1. Relationship between moisture content and time during hydration [41].

value after initial hydrolysis period, the hydration is the most violent, and this moment can be regarded as the final setting state moment.

The ideal situation for concrete setting allows sufficient time to complete the construction process of mixing, transporting, pouring, vibrating and plastering, while having a short final setting period for early demolding, rapid hardening, and using. Hydration is a decisive factor during the curing process of concrete. The curing condition timing should be adjusted according to the monitored setting state of the concrete. The goal is to ensure that concrete fabrication complies with the construction standards. Therefore European and American standards stipulate that cement's initial setting time should not be earlier than 45 min, and the final setting time should not be more than 10 h [43].

Cement often has a pre-hydration effect before it is mixed with other materials. When cement is in contact with air, it will absorb the air's water vapor. Factories produce cement by grinding clinker and gypsum. The gypsum will be dehydrated and release water that may react with the clinker. In addition, cement manufacturers also add 2% water to the machine to reduce the equipment's temperature while it is working. These conditions prevent the cement from becoming completely dry. The primary effects of cement pre-hydration on engineering performance is the prolongation of setting time, the change in compressive strength, and its rheological properties [44,45]. Significantly, the pre-hydration of cement paste in air and the initial reaction ratio of cement at the beginning of the experiment may affect measurement results. The authors of this paper carried out preliminary experiments to investigate the effects of pre-hydration and the initial reaction ratio of cement to the water content of paste.

3. Detection mechanism

The dielectric constant of the medium will affect the transmission time and amplitude of the reflected signal in GPR. In this section, we characterize the relationship between the cement paste composition and the dielectric constant. Furthermore, we judge the setting state of the cement paste through the change of moisture content during the hydration process to detect its setting time. Eventually, the relationship between the moisture content and the setting state is converted into the relationship between the electrical parameters to be measured and the setting state.

The dielectric constant of cement paste varies with the moisture content, temperature, cement type, admixture, and ion concentration. According to Refs. [46,47], the composition of cement paste has less influence on the dielectric constant than water content. The dielectric constant of ordinary concrete largely depends on the water content. Generally speaking, the dielectric constant of a material increases with increasing temperature. In the curing of cement, the effect of temperature on water is mainly the water evaporation caused by heating rather than the dielectric constant of water. Moreover, the dielectric constant of ordinary concrete remains basically unchanged from 275 K (1.85 °C) to 380 K (106.85 °C) [48]. In this article, ordinary Portland cement (OPC) was used to make cement paste for experiments. Since no cement admixture is added, the influence of ion concentration in the solution can be ignored and since the experiment was maintained at a 20 °C ambient environment, the temperature effect on the dielectric constant can be ignored.

The key electrical characteristic that reflects cement paste composition is the dielectric constant. Ground penetrating radar is used to monitor the electrical properties of cement paste to obtain material composition and determine the setting state of cement paste. The change in moisture content, which is reflected by the change in dielectric constant, can be employed to determine the setting state. Therefore, the setting state can be determined by a change in the dielectric constant.

3.1. The relationship of moisture content and dielectric constant

Cement paste is a type of composite material. The dielectric constant of composite material can be calculated by combining the dielectric constant of its components according to its empirical formula. Birchack's theory can be used to compute the dielectric constant of composite materials [49]. According to the Birchack's theory, we can use the following Equation (1)&2 to calculate the dielectric constant of cement paste:

$$\varepsilon^{\alpha} = f_1\varepsilon_{fw}^{\alpha} + f_2\varepsilon_{cw}^{\alpha} + f_3\varepsilon_{solid}^{\alpha} + f_4\varepsilon_{air}^{\alpha} \tag{1}$$

$$f_1 + f_2 + f_3 + f_4 = 1 \tag{2}$$

The dielectric constants of concrete materials are shown in Table 1:

In Table 1, ε_{fw} ε_{cw}, ε_{solid}, and ε_{air} are the dielectric constant of free water, bound water, cement gels, and air, respectively [50]. α is an experimentally determined value of 0.5.

Cement paste is less complicated than concrete in terms of composition and nature. Free water plays a major role in calculating the dielectric constant of cement paste. To highlight the effect of free water, we can divide cement paste into two parts, free water and other components. The calculation formula of the dielectric constant of cement paste is shown in Eq. (3).

$$\varepsilon^{\alpha} = f_1\varepsilon_{fw}^{\alpha} + f_5\varepsilon_{\text{other}}^{\alpha} \tag{3}$$

Table 1
Parameters of the cement paste, i.e. the dielectric constants.

Parameters	ε_{cw}	ε_{fw}	ε_{solid}	ε_{air}	α
Values	4	82	4	1	0.5

$$f_1 + f_5 = 1 \tag{4}$$

In Eqs. (3) and (4), ε_{other} andf_5 are the dielectric constant and volume fraction of other components, respectively. In Fig. 2, the dielectric constant of the cement paste linearly varies with the free water content. We can use the dielectric constant change to describe the moisture content change.

3.2. The relationships between moisture content, dielectric constant and setting time

The moisture content of the cement paste in an actual construction site is often not directly measured, and the measured relevant parameters (resistance, dielectric constant, etc.) are used to characterize the moisture content. The changing characteristics of the dielectric constant during the setting process are similar to the moisture content. Therefore, this paper uses it to express the changing acceleration of the moisture content to determine the cement paste's setting time. The change in dielectric constants and moisture content over time can be represented in Fig. 3.

3.3. The principle of GPR

GPR is a complex system with three components: signal transmitting, data analysis, and signal receiving, as shown in Fig. 4.

In Fig. 4, θ_0, θ_3, and θ_4 are the incident angles of an electromagnetic wave incident on each medium stratification plane. θ_1 and θ_2 are the incident angle of the electromagnetic wave on each medium stratification plane. A_1, A_2, and A_3 represent the echo intensity of each layer. Then, ε_0, ε_1, ε_2, and ε_3 refer to the dielectric constant of air, surface layer, base layer, and subgrade, respectively.

GPR modulates high-frequency electromagnetic waves in a solid cavity and then sends them to a dielectric surface by a radiator. Electromagnetic waves penetrate through and reflect on interfaces with different impedances. Engineers can obtain the target's characteristic information by analyzing time spectrum characteristics and amplitude of the reflected electromagnetic wave signal.

The dielectric constant of the medium is a principal factor affecting electromagnetic wave propagation. It is expressed as the ratio of the dielectric constant to the medium to the vacuum dielectric constant (8.854×10^{-9} F/m), namely the relative dielectric constant, which is often referred to as the dielectric constant without the prefatory "relative."

$$\varepsilon_r = \frac{\varepsilon}{\varepsilon_0} = \varepsilon_r^{'} - j\varepsilon_r^{''} \tag{5}$$

where $\varepsilon_r^{'}$ is the real part of dielectric constant, and $\varepsilon_r^{''}$ is the imaginary part of the dielectric constant. The real part represents the storage effect of the medium on electromagnetic waves. The imaginary part reflects the loss characteristics of the medium to the electromagnetic waves. The imaginary part of concrete dielectric constant can go as high as 2.2, which incurs a serious loss to electromagnetic wave propagation. Due to the attenuation of electromagnetic waves in the medium, the lower the electromagnetic frequency emitted by GPR; moreover, the greater the depth of detection in the medium, the lower the resolution (the minimum size that can be distinguished). Conversely, the detection depth of high-frequency electromagnetic waves in the medium is smaller than that of low-frequency electromagnetic waves, but the measurement resolution is higher, which means it can detect thin layers. Therefore, a tradeoff exists between the detection depth of electromagnetic waves and the resolution of GPR.

3.4. Full-waveform inversion method

3.4.1. Definition of the generalized reflection coefficient

Cement paste is considered to be homogenous and isotropic for the sake of theoretical computation. Then, the propagation of electromagnetic waves in cement paste is related to the characteristics of the electromagnetic wave itself and the properties of the

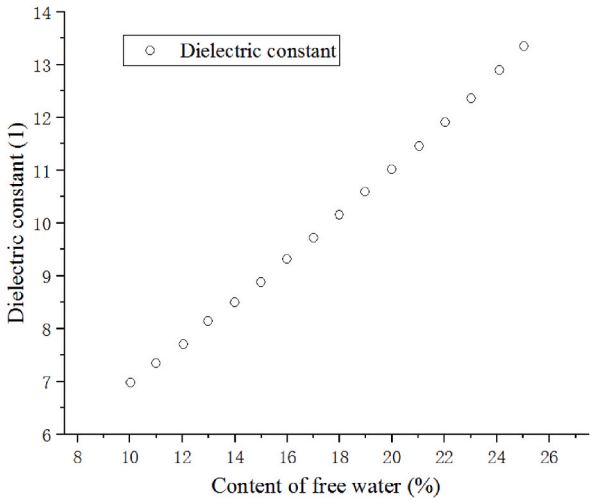

Fig. 2. Relationship between free water change and dielectric constant of cement paste [15].

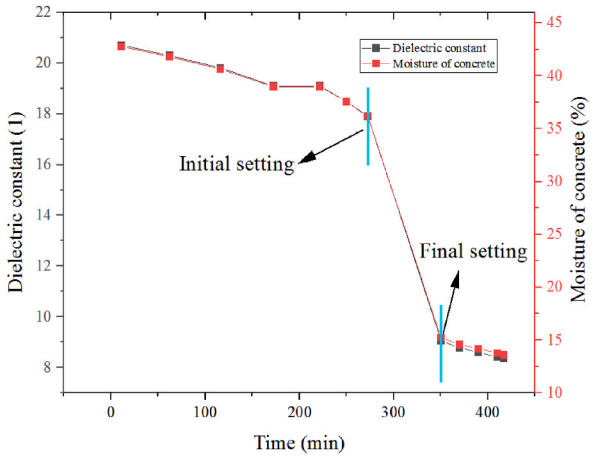

Fig. 3. Relationship among moisture content, dielectric constant, and setting time during hydration [15].

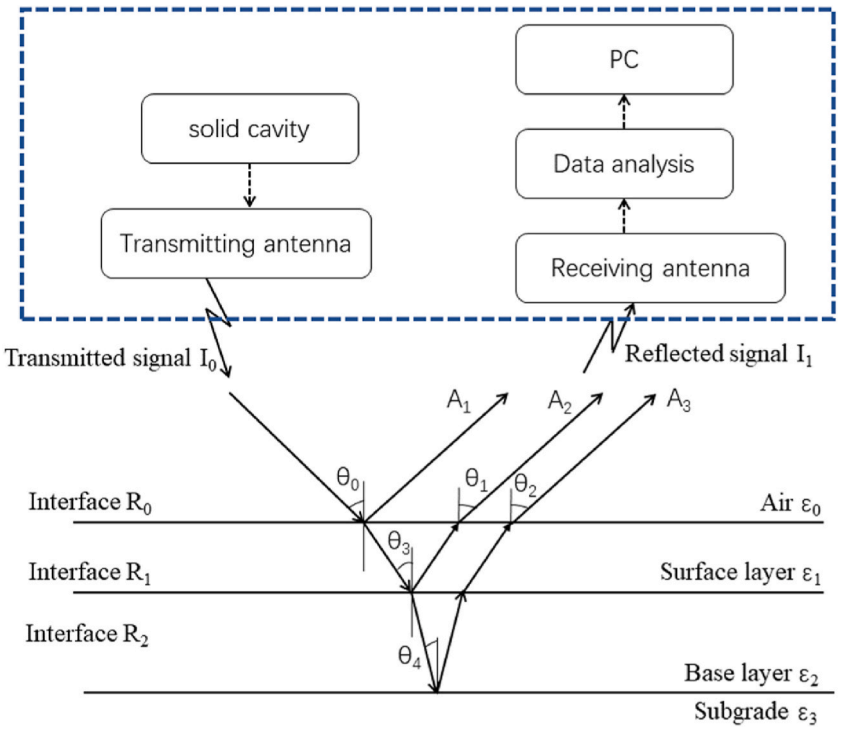

Fig. 4. GPR system and working principle.

medium material, which is usually described by the propagation constant:

$$\gamma = \beta - j\alpha \tag{6}$$

where α is the attenuation constant, and β is the phase constant. Thus, α and β can be expressed as:

$$\begin{cases} \alpha = \omega\sqrt{\dfrac{\mu\varepsilon}{2}\left[\sqrt{1+\left(\dfrac{\sigma}{\omega\varepsilon}\right)^2}-1\right]} \\ \beta = \omega\sqrt{\dfrac{\mu\varepsilon}{2}\left[\sqrt{1+\left(\dfrac{\sigma}{\omega\varepsilon}\right)^2}+1\right]} \end{cases} \tag{7}$$

where ω,ε,σ and μ represent angular frequency, dielectric constant, electrical conductivity and magnetic permeability, respectively.

Generally, by defining the reflection coefficient and projection coefficient on the interface of the i_{th} layer, the reflection coefficient r and the transmission coefficient τ of the interface between the i layer and the $i+1$ layer, which can be written as:

$$\begin{cases} r_{i,i+1} = (\eta_{i+1} - \eta_i)/(\eta_{i+1} + \eta_i) \\ \tau_{i,i+1} = 2\eta_{i+1}/(\eta_{i+1} + \eta_i) \end{cases} \tag{8}$$

where $\eta_i = \sqrt{\frac{j\omega\mu}{\sigma+j\omega\varepsilon}}$. The cement paste is regarded as a non-magnetic nondestructive medium. Then, to facilitate the subsequent calculation of the dielectric constant and better understand the propagation of electromagnetic waves in the medium, we calculated the following:

$$r_{i,i+1} = \frac{\sqrt{\varepsilon_i} - \sqrt{\varepsilon_{i+1}}}{\sqrt{\varepsilon_i} + \sqrt{\varepsilon_{i+1}}} \tag{9}$$

where ε_i and ε_{i+1} are the dielectric constants of the i_{th} and$i+1_{th}$ layers, and $r_{i,i+1}$ is the reflection coefficient between the two layers.

We defined the ratio of the reflected wave amplitude to the emitted wave at the interface of each layer as the generalized reflection coefficient denoted as R. Since there is air above the top of the first layer, there is $R_{01} = r_{01}$. The i_{th} generalized reflection coefficient can be deduced as:

$$R_{i,i+1} = r_{i,i+1} \prod_{k=0}^{i-1} \left(1 - r_{k,k+1}^2\right) \prod_{k=1}^{i} e^{-2\alpha_k d_k} \tag{10}$$

where α_k is the attenuation constant, andd_k is the thickness of the k_{th} layer.

3.4.2. Calculation of dielectric constant

In general, the dielectric constant of the dielectric layer can be calculated directly from Eq. (7). Al-Qadi et al. [25] proposed a method using a full-waveform inversion. Eq. (11) is used to calculate the dielectric constant ε_1 of the first layer:

$$\varepsilon_1 = \left[\frac{1 + \left(\frac{A_0}{A_{inc}}\right)}{1 - \left(\frac{A_0}{A_{inc}}\right)}\right]^2 \tag{11}$$

where A_0 is the amplitude of the reflected wave at the first layer, andA_{inc} is the amplitude of the transmitted signal. Total reflection effect can be generated when a GPR pulse wave reaches the metal plate. Thus, the amplitude received by the antenna is the same as that of the transmitted signal.

The dielectric constant of the second layer can be obtained from the calculated formula of the reflection coefficient and the correction of transmission loss.

$$\varepsilon_2 = \varepsilon_1 \left(\frac{1 - r_{01}^2 + R_{12}}{1 - r_{01}^2 - R_{12}}\right)^2 = \varepsilon_1 \left\{\frac{1 - [A_0/A_{inc}]^2 e^{-\eta_0 \frac{\sigma_1 t_1 c}{2\varepsilon_1}} + [A_1/A_{inc}]^2}{1 - [A_0/A_{inc}]^2 e^{-\eta_0 \frac{\sigma_1 t_1 c}{2\varepsilon_1}} - [A_1/A_{inc}]^2}\right\}^2 \tag{12}$$

where t_1 and σ_1 represent the two-way travel time and conductivity of the first layer, respectively, A_1 is the amplitude of the reflected wave at the second layer. Thus, the modified formula is extended to multiple layers and is expressed as:

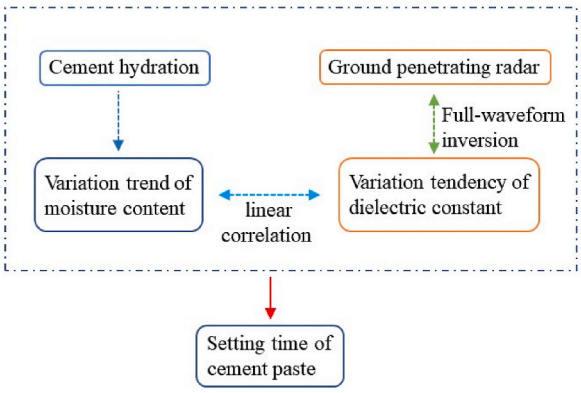

Fig. 5. Theoretical route of GPR monitoring method.

$$\varepsilon_n = \varepsilon_{n-1}\left(\frac{1 - r_{01}^2 + \sum_{i=1}^{n-2} r_{i-1,i}R_{i,i+1} + R_{n-1,n}}{1 - r_{01}^2 + \sum_{i=1}^{n-2} r_{i-1,i}R_{i,i+1} - R_{n-1,n}}\right)^2 \tag{13}$$

Full-waveform inversion has previously been adopted by United States Departments of Transportation to apply to pavement moisture accumulation localization [51–53]. In practice, the measured objects are often not a uniform monolayer medium. The dielectric constant of cement paste can also use the preceding formulas in later experimental processing of this research. Finally, the methodology of the detection method and relationship between the parts can seen in Fig. 5.

4. Simulation in HFSS

The measurement principle for the full-waveform inversion method is to judge the state of the medium by comparing the intensity of the collected signals. The strength of the reflected signal is not only related to the signal intensity of GPR itself, but also related to the electrical parameters of the medium. The greater the intensity of the initial emitted electromagnetic signal, the stronger the reflected signal received, and the greater the echo amplitude. In addition, the higher the electrical parameter of the medium (usually referring to the dielectric constant of the medium), the greater the reflection coefficient S_{11} of the electromagnetic wave, and the stronger the reflected signal [54].

In this section, the Ansoft High Frequency Structure Simulator (HFSS) is used to analyze the interaction between the echo strength of electromagnetic waves and the dielectric constant of the medium. The electromagnetic wave emitted by GPR can be regarded as a plane wave, and the incidence mode is usually a vertical incidence. To explore the relationship between the dielectric constant of the medium and the echo strength of the signal, the incidence of electromagnetic waves of various frequencies into a material whose permittivity varies is simulated in HFSS. Commercial GPR antennas are often transceiver integrated, which means the GPR transmitting and receiving antennas are in the same detector. There is a shielding shell between them so that the two antennas will not affect each other during measurement. Fig. 6 shows the HFSS model. The dielectric constant variable medium is below the air layer, while the electromagnetic wave emitting and receiving end is above it. The distance between the cement paste and the emitting terminal should be greater than at least 1/4 wavelength to ensure the calculation accuracy of far-field radiation. The transmitting port is set as the Floquet port, and the medium boundary is set as the master and slave boundary. The medium was configured as a substance with electrical properties comparable to concrete. The relative permeability is 1, and the dielectric loss tangent is 2.2.

According to the measurement of the SIR-4000 GPR antenna, the central frequency is 1.6 GHz, and the electromagnetic wave band of 1.2–1.9 GHz is simulated in the HFSS. The simulation results show that the reflection coefficient S_{11} increases with the increase of the dielectric constant of the medium. Fig. 7 depicts the simulated pattern diagram of the reflection coefficient and the dielectric constants as an echo amplitude and dielectric constant changes. The simulation results show that the influence of electromagnetic waves of different frequencies on the measurement of the reflection coefficient S_{11} is tolerable, which indicates that GPR will not be affected by the frequency of electromagnetic waves when measuring the dielectric constant.

In the solid resonant cavity, the broadband high frequency electromagnetic wave modulated by GPR is normally dispersed around the antenna central frequency, with the low frequency being greater than the high frequency. When the central antenna frequency is 1.6 GHz, the simulation sweep frequency is adjusted at 1.2–1.9 GHz to come near to the actual condition. When the medium's dielectric constant stays constant, the reflection coefficient in the GPR working band for the medium varies little and remains steady, as seen in Fig. 7. The dielectric constant and reflection coefficient has a nearly linear pattern, which is compatible with using higher frequency electromagnetic waves in GPR to defect the smallest recognition sizes in detection.

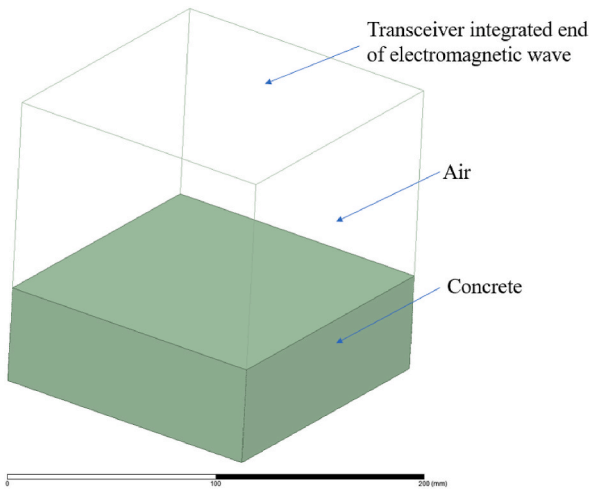

Fig. 6. The simulation model in a high frequency structure simulator (HFSS).

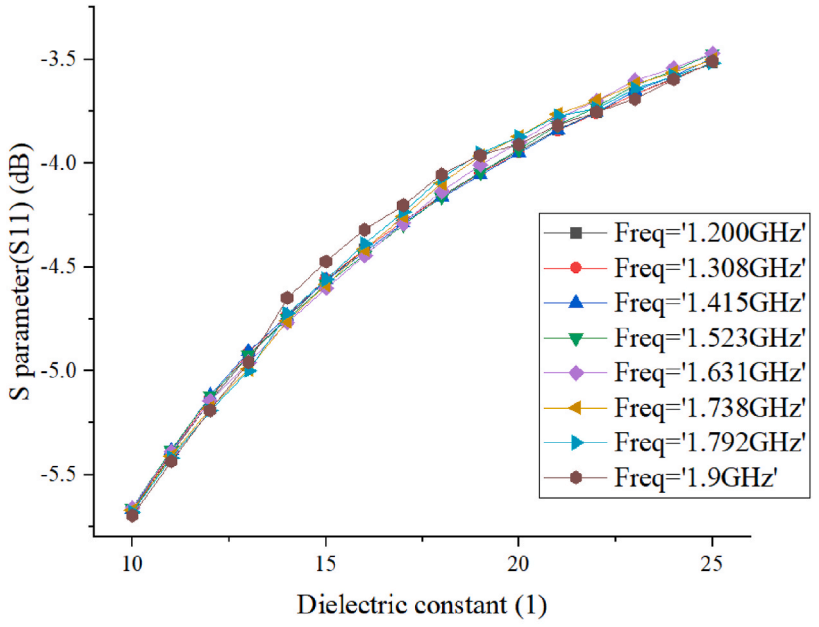

(a)

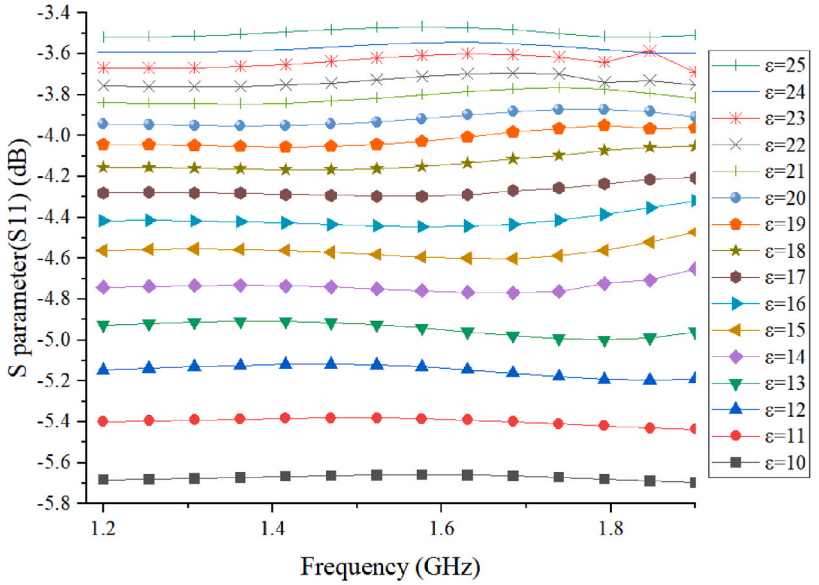

(b)

Fig. 7. Relationship between the (a) dielectric constant of the medium and (b) the reflection coefficient S_{11} in different frequencies.

5. Experiments and analyses

5.1. Experimental scheme and design

Some water and cement immediately combined to generate hydration products and accompanied by the release of a large amount of heat, which will also lead to direct evaporation of some water. The ratio of the water consumed immediately to the initial amount of

water added is the initial reaction ratio of the cement hydration. In this paper, the initial water reaction ratio of cement paste was measured in advance before the experiment. The experimental results show that the initial reaction ratio of water is about 27.6%, which is close to the initial change of the water content measured by Ref. [55]. The bound water formed by hydration and the free water are defined as two materials with varying permittivity in the theoretical computation of permittivity. As a result, while calculating the dielectric constant of cement paste theoretically at the start of the experiment, the contribution of the initial mix ratio and first reaction ratio should be taken into account simultaneously.

The OPC used in this experiment was first dried in an oven, then the initial reaction ratio was determined. Furthermore, to ensure that GPR can be used to monitor cement paste setting time in all situations, a preliminary test was performed to determine if the water cement ratio in a certain range has an effect on the setting time of cement paste.

The full-waveform inversion method requires that the measurement height is appropriate and the distance of each measurement is fixed. This paper adopts the SIR-4000 GPR with a 1600-Mhz operating antenna for a continuous 12 h of fixed measurement distance detection for $140 \times 140 \times 50$ mm^3 cement paste. The experimental facilities are shown in Fig. 8. The cement paste mixed at the same time was tested by the Vicat apparatus, and the measurement results were taken as the control group and compared with the GPR test results. Each group of experimental samples are measured every 10 min in the first 3 h, and multiple groups of echo data were recorded at one time. Three hours later, the interval time of each measurement group was shortened to 5 min.

5.2. Analysis and interpretation of experimental results

In this paper, analysis was conducted based on the experimental results of the Vicat apparatus first and then, the GPR inversion. The experimental results of each group are shown as follows. The initial reaction rate of the cement used is 30%, which will be considered in the follow-up analysis of experimental data for moisture content monitoring.

5.2.1. Vicat apparatus test

The Vicat measurement is to judge the setting state of cement paste by the penetration depth of Vicat. In this experiment, the penetration depth measured by Vicat apparatus on the surface of the cement paste test is shown in Fig. 9. According to the Standard Schema in EN 13294–2002 [43,56], when the cement paste reaches the initial setting state, the penetration depth of Vicat will decrease from 67 to 65 mm. The initial setting time of the cement tested by the Vicat apparatus in this paper was 282 min or 4 h and 42 min (4.70 h). The final setting time was 450 min or 7 h and 30 min (7.5 h).

5.2.2. Analysis of GPR experimental data

Sixty sets of echo data were recorded during a single GPR measurement (two sets of cement paste samples, with an average of 30 sets of data measured in each group). After screening and excluding abnormal data caused by an abnormal measurement operation, the average value is taken as the experimental data of each time to ensure the universality of the experiment. Then, the full-waveform inversion method is used to calculate the dielectric constant of cement paste as we observe its setting state.

The following is a calculation example. Fig. 10 shows the echo information of the metal plate and cement paste at the same distance. Since the detection antenna is not very close to the target surface, *ADw* is obviously the direct wave, which is the first wave energy propagated from a transmitter antenna to reach a receiver antenna. A_{inc} and A_0 are the echo amplitude of metal plate and cement paste, respectively. They are used to calculate the dielectric constant of the sample by full-waveform inversion method.

The dielectric constant, ε_1, of cement paste is calculated as:

$$\varepsilon_1 = \left[\frac{1 + \left(\frac{A_0}{A_{inc}}\right)}{1 - \left(\frac{A_0}{A_{inc}}\right)}\right]^2 = 35.2307 \tag{14}$$

The dielectric constant, ε_0, of the air is known as 1, so we can calculate the reflection coefficient, r_{01}.

Fig. 8. GPR Experiment measurement.

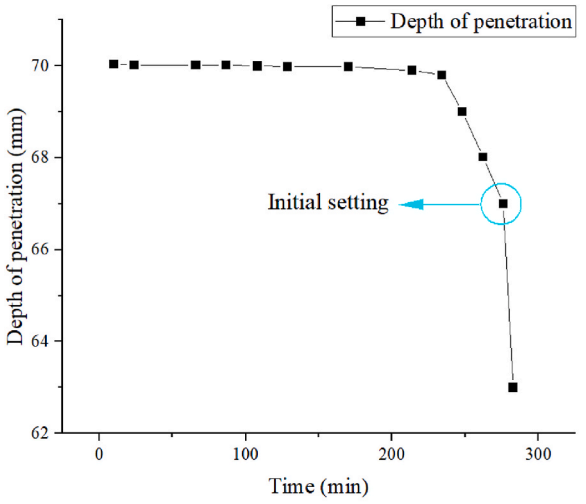

(a)

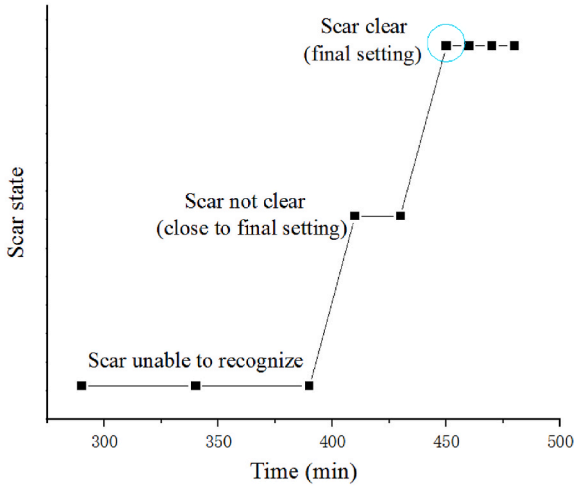

(b)

Fig. 9. Vicat apparatus testing: (a) initial setting and (b) final setting.

$$r_{01} = \frac{\sqrt{\varepsilon_0} - \sqrt{\varepsilon_1}}{\sqrt{\varepsilon_0} + \sqrt{\varepsilon_1}} \tag{15}$$

In Equation (15) we obtain the reflection coefficient of first layer, r_{01}. By using measured echo amplitude, A_1, to get the generalized reflection coefficient, R_{12}, we can then obtain the second layer of the dielectric constant.

$$\varepsilon_2 = \varepsilon_1 \left(\frac{1 - r_{01}^2 + R_{12}}{1 - r_{01}^2 - R_{12}} \right)^2 = \varepsilon_1 \left\{ \frac{1 - r_{01}^2 + [A_1/A_{inc}]^2}{1 - r_{01}^2 - [A_1/A_{inc}]^2} \right\}^2 \tag{16}$$

After processing the measured echo data, the inversion results show the dielectric constant of cement paste to be basically unchanged at the beginning. Still, there is a slight trend of decline. With the end of the initial setting period, the hydration of the cement paste entered the accelerated period, which means hydration accelerated, moisture content decreased rapidly and the dielectric

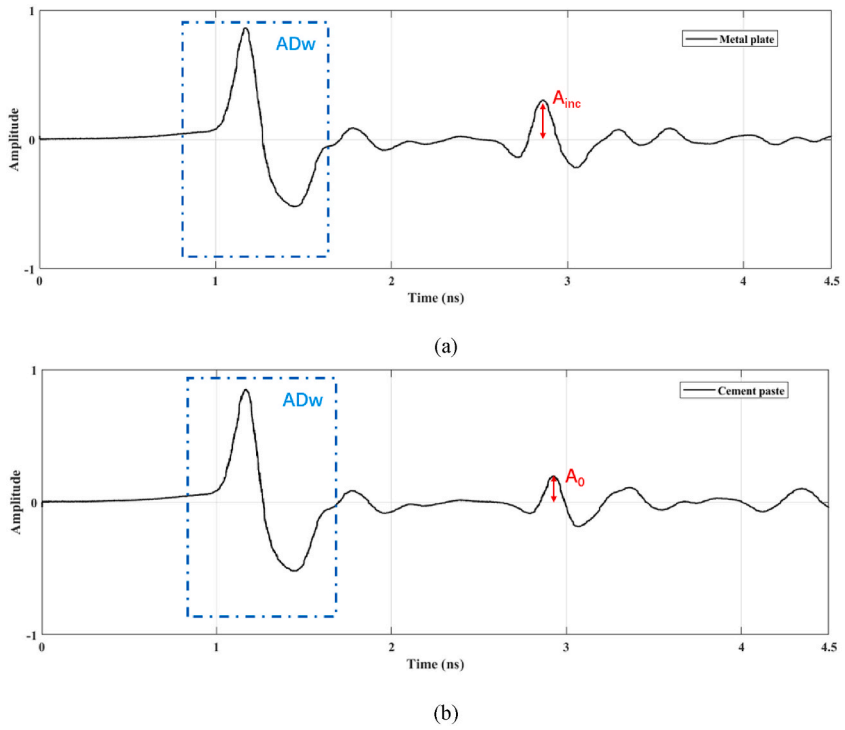

Fig. 10. GPR testing: (a) the echo information of a metal plate and (b) the echo information of cement paste.

constant also decreased rapidly. Finally, after the end of the acceleration period, the deceleration period began and the changes in the dielectric constant of the cement paste gradually leveled off. The dielectric constant remained nearly constant at this time. The variation trend of the dielectric constant of the cement paste is similar to a tensile Z character, as shown in Fig. 11. The results of the data in the figure are similar to those of the previous study [15].

The results of echo information inversion monitored in this experiment can describe the changing moisture content trend of cement paste. The dielectric constant of cement paste is linearly related to its moisture content, so the changing cement paste trend of the dielectric constant can be used to characterize the changes in its moisture content. We can judge the setting time of cement paste by fitting the acceleration of water content change. The initial setting time is considered as the time when the dielectric constant (moisture content) begins to decrease rapidly. As can be seen from Fig. 11, the initial setting time of the first group was 310 min (5 h and 10 min), and the second group was 300 min (5 h).

In the process of measurement, the cement paste is sampled and analyzed regularly. The relationship between the dielectric constant (moisture content) and time is shown as a set of scattered data. Any change in moisture content is a derivative of the moisture content curve. In this paper, the curve representing the changes in the dielectric constant of cement paste is used to describe the changes in moisture content. The rate of change is often measured by the derivative or differential of the curve at some point. For scatter data, the differential of the dielectric constant at time T (point n) is often calculated with a certain length of time window. The time window of differential calculation generally starts from the first k points of the calculation point and ends at the last k points of the point. By calculating the slope of the line segment fitted by these points, the slope can be regarded as the derivative of the intermediate points with respect to time, which is also the acceleration of the changes in the dielectric constant (moisture content).

In this paper, the setting state of cement paste is judged by the slope (the acceleration of the dielectric constant) fitted with the time window data of a certain length. In the experimental results, the time window length adopted by multiple data processing is changed in a certain range. In the end, 10 consecutive points were selected as the sampling time window length (the results of 7 and 11 discrete points were similar), and the time point of the final setting was the time when the derivative of the dielectric constant with time was maximum (i.e., the acceleration of the change in water content was maximum).

The data of the dielectric constant obtained in the experiment were fitted to obtain the derivative. Finally, the relationship between the change rate of the dielectric constant at each point and the time during the measurement period is shown in Fig. 12. The extreme point of the dielectric constant after initial setting, that is the final setting time of cement paste, has been marked in Fig. 12. The final setting time of each experimental group was 480 min (8 h) for the first group, and 465 min (7 h and 39 min) for the second group. In addition, the time corresponding to the first peak in Fig. 12 is just close to the initial setting time. According to the experimental results, this paper believes that the change rate of the dielectric constant can be considered to determine the initial setting time point.

5.2.3. Data comparison of measurement results

The results of Vicat and GPR measurements are shown in Table 2. The average error of each set of measurements is also in this table.

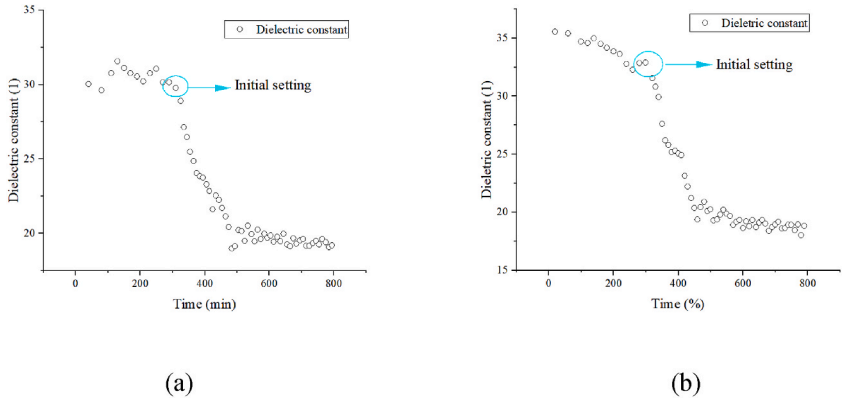

Fig. 11. Relationship between time and dielectric constant in (a) Group 1 and (b) Group 2.

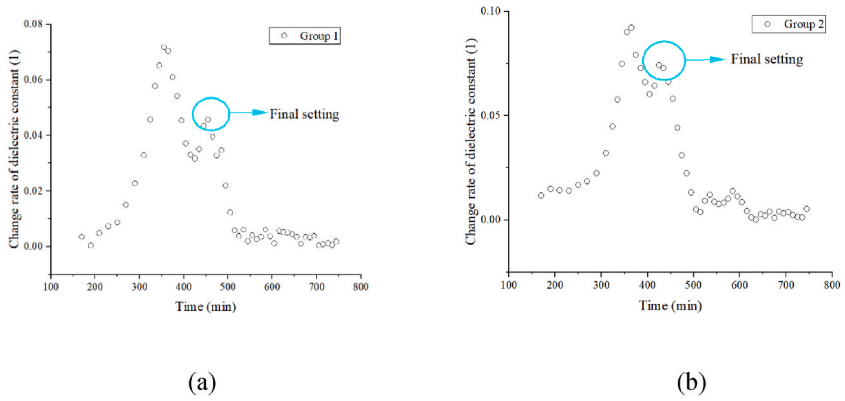

Fig. 12. Relationship between time and change rate of dielectric constant: (a) Group 1 and (b)Group 2.

The surface conditions of each group of samples were slightly different, but the initial and final setting times measured by GPR were similar to those measured by the Vicat apparatus. Because judging the setting state of cement paste by the change rate of dielectric constant (moisture content) can greatly reduce the influence of environmental noise (the effects of environmental noise can be regarded as a constant, which is zero after taking the derivative). The measurement errors of the initial setting time and the cement paste's final setting time are below 10%, and the average error of the three group is below 6%. For concrete, which is a material with great variability and uncertainty, the GPR measurement error results are tolerable, which also proves the good applicability of GPR in setting time measurement.

6. Conclusions and future research

This paper introduces a non-contact and remote sensing method using GPR to monitor the setting time of cement paste. Based on the characteristics of cement paste in the process of hydration and the sensitivity of the electromagnetic wave to water, a compound model based on equivalent dielectric constant and a simulation model based on HFSS were adopted to verify the feasibility of the experiment. Then, the positive correlation between reflection coefficient and dielectric constant is verified by simulation. Meanwhile, the simulation shows that the change of electromagnetic frequency has little effect on the reflection coefficient of the dielectric constant. Finally, the full-waveform inversion method was used to process the GPR measurement results. The dielectric constant measured by GPR was used as the index parameter of the moisture content of cement paste.

The setting time of cement paste was obtained by calculating the change rate of the dielectric constant. The final GPR measurement

Table 2
Comparison for the three experiment group.

Parameter	Vicat	Group 1	Group 2	Average	Error (%)
Initial setting time (min)	282	310	300	297.3	5.42%
Error (%)	/	9.92	6.38		/
Final setting time (min)	450	455	435	446.7	0.73%
Error (%)	/	1.11	3.33		/

result and the standard Vicat apparatus measurement result error is not more than 10%. In the actual measurement process, the setting time of cement paste is related to the change rate of the dielectric constant, and the effects of environmental noise can be ignored. The experiments indicate that GPR can be used to detect the setting time of cement hydration. Meanwhile, the experiments also demonstrate the possibilities of GPR in conjunction with construction automation. Automatic monitoring of cement setting state can be effectively linked with construction automation to assure the quality control of concrete during the building process, replacing the laborious process of artificially detecting the setting stage of concrete in engineering. Future research includes measurement distance calibration and distance self-compensation. The data processing methods for sensitivity enhancement were noted as the experimental and simulation results, respectively. They were reported to improve our understanding of the performance of cement after hardening.

CRediT authorship contribution statement

Liyu Xie: Conceptualization, Methodology, Writing - Original Draft, Writing - Review & Editing, Project administration, Funding acquisition. **Zihan Xia:** Conceptualization, Methodology, Formal analysis, Investigation, Writing - Original Draft, Writing - Review & Editing. **Songtao Xue:** Conceptualization, Supervision, Writing - Review & Editing. **Xiaoli Fu:** Formal analysis, Writing - Original Draft.

Funding

This research was funded by the National Natural Science Foundation of China (Grant Nos. 52178298 and 52078375), the Key Program for International S&T Cooperation Projects of China (No. 2021YFE0112200) and the Top Discipline Plan of Shanghai Universities-Class I.

Declaration of competing interest

The authors declare that they have no known competing financial interests or personal relationships that could have appeared to influence the work reported in this paper.

Data availability

Data will be made available on request.

References

[1] S. Mindess, J.F. Young, Prentice Hall, Concrete, 2002.
[2] Banfill PF. The rheology of fresh cement and concrete-a review. Proceedings of the 11th international cement chemistry congress2003. p. 50-62.
[3] W.-J. Liu, X.-J. Niu, N. Yang, Y.-S. Tan, Y. Qiao, C.-F. Liu, et al., Prediction model of concrete initial setting time based on stepwise regression analysis, Materials 14 (2021) 3201.
[4] R. Piyasena, P. Premerathne, B. Perera, S. Nanayakkara, Evaluation of initial setting time of fresh concrete, in: Proceedings of the 19th ERU Symposium, 2013, pp. 47–52.
[5] A.E. Abalaka, Effects of sugar on physical properties of ordinary Portland cement paste and concrete, AU JT 14 (2011) 225–228.
[6] Á. García, D. Castro-Fresno, J.A. Polanco, Maturity approach applied to concrete by means of Vicat tests, ACI Mater. J. 105 (2008) 445.
[7] L. Struble, T.Y. Kim, H. Zhang, Setting of cement and concrete, Cem. Concr. Aggregates 23 (2001) 88–93.
[8] C. Hao, L. Shi-liu, H. Yan-Ling, C. Jin, Principle and key technology of full automatic Vicat apparatus, in: Journal of Civil, Architectural & Environmental Engineering, 2015, pp. 92–96.
[9] S. Xue, Z. Yi, L. Xie, G. Wan, Double-frequency passive deformation sensor based on two-layer patch antenna, Smart Struct. Syst. 27 (2021) 969–982.
[10] S. Xue, K. Xu, L. Xie, G. Wan, Crack sensor based on patch antenna fed by capacitive microstrip lines, Smart Mater. Struct. 28 (2019), 085012.
[11] S. Sharma, A. Mukherjee, Longitudinal guided waves for monitoring chloride corrosion in reinforcing bars in concrete, Struct. Health Monit. 9 (2010) 555–567.
[12] Z.J. Li, L.Z. Xiao, X.S. Wei, Determination of concrete setting time using electrical resistivity measurement, J. Mater. Civ. Eng. 19 (2007) 423–427.
[13] N. Toropovs, F. Lo Monte, M. Wyrzykowski, B. Weber, G. Sahmenko, P. Vontobel, et al., Real-time measurements of temperature, pressure and moisture profiles in High-Performance Concrete exposed to high temperatures during neutron radiography imaging, Cement Concr. Res. 68 (2015) 166–173.
[14] A.M. She, K. Ma, G. Liao, W. Yao, J.Q. Zuo, Investigation of hydration and setting process in nanosilica-cement blended pastes: in situ characterization using low field nuclear magnetic resonance, Construct. Build. Mater. (2021) 304.
[15] Z. Yi, S. Xue, L. Xie, G. Wan, Detection of setting time in cement hydration using patch antenna sensor, Struct. Control Health Monit. (2021) e2855.
[16] G. Trtnik, G. Turk, F. Kavcic, V.B. Bosiljkov, Possibilities of using the ultrasonic wave transmission method to estimate initial setting time of cement paste, Cement Concr. Res. 38 (2008) 1336–1342.
[17] A.K. Khamzin, A.V. Varnavina, E.V. Torgashov, N.L. Anderson, L.H. Sneed, Utilization of air-launched ground penetrating radar (GPR) for pavement condition assessment, Construct. Build. Mater. 141 (2017) 130–139.
[18] Wei X, Zhou J, Zhang Y. Modified Compressive Sensing-Based Migration for GPR Probing of Reinforced Concrete Bridge Decks.
[19] M.A. Rasol, V. Pérez-Gracia, F.M. Fernandes, J.C. Pais, S. Santos-Assunçao, C. Santos, et al., GPR laboratory tests and numerical models to characterize cracks in cement concrete specimens, exemplifying damage in rigid pavement, Measurement 158 (2020), 107662.
[20] M.-S. Kang, N. Kim, J.J. Lee, Y.-K. An, Deep learning-based automated underground cavity detection using three-dimensional ground penetrating radar, Struct. Health Monit. 19 (2020) 173–185.
[21] P. Wiwatrojanagul, R. Sahamitmongkol, S. Tangtermsirikul, N. Khamsemanan, A new method to determine locations of rebars and estimate cover thickness of RC structures using GPR data, Construct. Build. Mater. 140 (2017) 257–273.
[22] I. Kaplanvural, E. Peksen, K. Ozkap, Volumetric water content estimation of C-30 concrete using GPR, Construct. Build. Mater. 166 (2018) 141–146.
[23] H. Liu, K. Takahashi, M. Sato, Measurement of dielectric permittivity and thickness of snow and ice on a brackish lagoon using GPR, Ieee J-Stars. 7 (2013) 820–827.
[24] I. Kaplanvural, K. Ozkap, E. Peksen, Influence of water content investigation on GPR wave attenuation for early age concrete in natural air-drying condition, Construct. Build. Mater. (2021) 297.
[25] I.L. Al-Qadi, S. Lahouar, Measuring layer thicknesses with GPR–Theory to practice, Construct. Build. Mater. 19 (2005) 763–772.
[26] M. Abouhamad, T. Dawood, A. Jabri, M. Alsharqawi, T. Zayed, Corrosiveness mapping of bridge decks using image-based analysis of GPR data, Autom. ConStruct. 80 (2017) 104–117.

[27] K. Rashid, R. Waqas, Compressive strength evaluation by non-destructive techniques: an automated approach in construction industry, J. Build. Eng. 12 (2017) 147–154.
[28] E. Saleh, A. Tarawneh, H. Dwairi, M. AlHamaydeh, Guide to non-destructive concrete strength assessment: homogeneity tests and sampling plans, J. Build. Eng. 49 (2022), 104047.
[29] J. Albers, S. Russell, K. Stewart, Concrete leveling techniques–a comparative ergonomic assessment, in: Proceedings of the Human Factors and Ergonomics Society Annual Meeting, SAGE Publications Sage CA, Los Angeles, CA, 2004, pp. 1349–1353.
[30] J. Zhang, J. Wang, S. Dong, X. Yu, B. Han, A review of the current progress and application of 3D printed concrete, Compos. Appl. Sci. Manuf. 125 (2019), 105533.
[31] M. Mishra, P.B. Lourenço, G.V. Ramana, Structural health monitoring of civil engineering structures by using the internet of things: a review, J. Build. Eng. 48 (2022), 103954.
[32] M. Gharbia, A. Chang-Richards, Y. Lu, R.Y. Zhong, H. Li, Robotic technologies for on-site building construction: a systematic review, J. Build. Eng. 32 (2020), 101584.
[33] B. Qi, M. Razkenari, A. Costin, C. Kibert, M. Fu, A systematic review of emerging technologies in industrialized construction, J. Build. Eng. 39 (2021), 102265.
[34] M. Xu, X. Nie, H. Li, J.C. Cheng, Z. Mei, Smart construction sites: a promising approach to improving on-site HSE management performance, J. Build. Eng. 49 (2022), 104007.
[35] D. Liu, Z. Li, J. Liu, Experimental study on real-time control of roller compacted concrete dam compaction quality using unit compaction energy indices, Construct. Build. Mater. 96 (2015) 567–575.
[36] W. Xu, Control Method of Concrete Layered Construction Based on Water State in Former Layer, Tsinghua University Beijing, China, 2017.
[37] K.J. Akram, T. Islam, A. Ahmed, A simple method on transformer principle for early age hydration monitoring and setting time determination of concrete materials, IEEE Sensor. J. 18 (2018) 7265–7272.
[38] K.J. Akram, A. Ahmed, T. Islam, Fringing field impedance sensor for hydration monitoring and setting time determination of concrete material, Ieee T Instrum Meas 69 (2019) 2131–2138.
[39] D.P. Bentz, A review of early-age properties of cement-based materials, Cement Concr. Res. 38 (2008) 196–204.
[40] H.F. Taylor, Cement Chemistry, Thomas Telford London, 1997.
[41] J. Pavlik, V. Tydlitat, R. Cerny, T. Klecka, P. Bouska, P. Rovnanikova, Application of a microwave impulse technique to the measurement of free water content in early hydration stages of cement paste, Cement Concr. Res. 33 (2003) 93–102.
[42] W. Xu, Q. Li, Y. Hu, Water content variations in the process of concrete setting, J. Hydroelectr. Eng. 36 (2017) 92–103.
[43] code Bb. British Standard for the Design and Construction of Reinforced and Prestressed Concrete Structures. BS 8110.
[44] E. Dubina, L. Black, R. Sieber, J. Plank, Interaction of water vapour with anhydrous cement minerals, Adv. Appl. Ceram. 109 (2010) 260–268.
[45] J. Wang, J. Xie, Y. Wang, Y. Liu, Y. Ding, Rheological properties, compressive strength, hydration products and microstructure of seawater-mixed cement pastes, Cement Concr. Compos. 114 (2020), 103770.
[46] T. Sokoll, A.F. Jacob, In-situ moisture detection system with a vector network analyser, Meas. Sci. Technol. 18 (2007) 1088–1093.
[47] X.M. Wang, Y.H. Teo, W.K. Chiu, G. Foliente, Evaluation of moisture content in concrete with microwave, Fracture of Materials: Moving Forwards 312 (2006) 311–318.
[48] B. Chambers, C.A. Pickles, P.J. Tumidajski, Temperature dependencies of the permittivities and microwave shielding effectiveness of a carbon-containing electrically conductive concrete, High Temp Mat Pr-Isr. 32 (2013) 427–435.
[49] J.R. Birchak, C.G. Gardner, J.E. Hipp, J.M. Victor, High dielectric constant microwave probes for sensing soil moisture, Proc. IEEE 62 (1974) 93–98.
[50] Z. Sun, Estimating volume fraction of bound water in Portland cement concrete during hydration based on dielectric constant measurement, Mag. Concr. Res. 60 (2008) 205–210.
[51] K.T. Tran, J. Sperry, Application of 2D full-waveform tomography on land-streamer data for assessment of roadway subsidence, Geophysics 83 (2018) EN1–EN11.
[52] A. Loulizi, Development of Ground Penetrating Radar Signal Modeling and Implementation for Transportation Infrastructure Assessment, Virginia Polytechnic Institute and State University, 2001.
[53] W.W.-L. Lai, X. Dérobert, P. Annan, A review of ground penetrating radar application in civil engineering: a 30-year journey from locating and testing to imaging and diagnosis, Ndt&E Int. 96 (2018) 58–78.
[54] R. Manchiryal, N. Neithalath, Electrical property-based sensing of concrete: influence of material parameters on dielectric response, Spec. Publ. 252 (2008) 23–40.
[55] J. Hu, Z. Ge, K. Wang, Influence of cement fineness and water-to-cement ratio on mortar early-age heat of hydration and set times, Construct. Build. Mater. 50 (2014) 657–663.
[56] code Eb. Products and systems for the protection and repair of concrete structures - test methods - determination of watertightness of injected cracks without movement in concrete. prEN 14068-2003.